Application of Axial Transmission technique to shear wave evaluation in bone with periostitis.

せん断波の Axial Transmission 法による炎症骨の評価

Kazuki Miyashita[1†], Mineaki Takata[1],Takashi misaki[1], Ko Chiba[2], Hiroshi Mita[2], Norihisa Tamura[2],and Mami Matsukawa[1] ([1]Doshisha Univ., [2]Nagasaki Univ. , [3]JRA Equine Research Institute.)

宮下和輝 [1†]，高田峰聖 [1]，見崎貴史 [1]，千葉恒 [2]，三田宇宙 [3]，田村周久 [3]，松川真美 [1]

([1] 同志社大, [2] 長崎大, [3]JRA 競走馬総合研究所)

1. Introduction

Evaluation of bone inflammation is very important for racehorses. The present mainstream of bone evaluation is X-ray techniques, which however is difficult to diagnose large animals. Therefore, development of safe and inexpensive quantitative ultrasound (QUS) techniques is expected [1]. One of the QUS methods, the Axial Transmission (AT) technique, offers the potential to estimate both mineral density and elastic properties of cortical bone [2]. Because the cortical bone supports the body load, fractures of this bone directly decreases the quality of life. The AT technique mostly measures the first arriving signal (FAS) which is a leaky wave from the bone surface. However, FAS velocity is highly dependent on cortical bone thickness and the shape of surface. Therefore, we next focused on the shear wave. Shear waves are related to the shear modulus and torsional strength which are also important factors of bone fracture.

In this study, we investigated the applicability of AT technique to shear wave evaluation in the horse leg bone by simulation. Here, the heterogeneity and anisotropy of horse bone were considered in the bone model, in addition to partial changes of velocity and structure due to inflammation.

2. 2D model construction

A 2D digital equine bone model was created from High Resolution - peripheral Quantitative Computerized Tomography (HR-pQCT) images of the third metacarpal bone with periostitis (100 months old). Figure 1 shows a cross section view of the bone model. The spatial resolution of the model was 61 μm. The local bone mineral densities were in the range from 920 to 1570 kg/m^3. The densities in the inflamed part were lower than those in the normal part.

The wave velocities in the axial direction were in the range of 3550 to 4280 m/s, which were measured by the ultrasonic pulse technique in the MHz range [3]. The velocities in the inflamed part were lower than those in the normal part. For simulation, the measured velocity distribution with a spatial resolution of 3 mm was interpolated to 61 μm using a bilinear interpolation [4]. To estimate all constants in all positions, we assumed that the Poisson's ratio was 0.33 [5] and referred to studies of Nakatsuji and Yamato [6,7]. Then, elastic constants changed due to the site. The shear wave velocities in the axial direction were in the range of 1790 to 2160 m/s. The averaged wave velocities were 1810 m/s in the inflamed part, 2070 m/s in the normal part. Table 1 shows one example of wave velocities in three directions in bone.

3. Simulation conditions

A 2D elastic finite-difference time-domain (FDTD) method was used [8]. Using an axial transmission configuration, transducers were set at incident angles of 60º keeping the same geometries shown in Fig. 2 [9]. A vacuum area was set between the transducers to avoid direct waves. The bone model was set in a water area for simulating the soft tissue. Longitudinal wave velocity and density in water were 1500 m/s and 2000 kg/m^3, respectively. The Higdon's second order absorbing boundary condition was applied. The input signal was one cycle of sinusoidal wave at 1 MHz with Hann window.

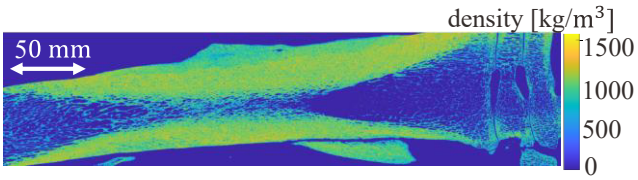

Figure 1 A cross section view of the 2D equine bone model.

Table 1 One example of wave velocities in the model.

	Longitudinal [m/s]	Shear [m/s]
Axial	4250	2140
Radial and Tangential	3470	1750

4. Results and discussion

One shot of wave propagation at 40 μs is shown in Fig. 3. The wave front I is the shear wave, and II is the longitudinal wave. The signals obtained at all receivers were stacked and shown as the B-scan image in Fig. 4. The wave front of longitudinal waves curved due to shape of bone surface. Figure 5 shows longitudinal and shear wave velocities estimated from the arrival time differences between adjacent receivers. The wave velocities observed by receivers 1-11 and 48-60 show the wave velocity in normal part, the wave velocities observed by other sensors 12-47 show the low shear wave velocities in inflamed part. The longitudinal wave velocities dramatically changed due to the shape of bone surface. However, the shear wave velocities did not show clear dispersion. In this simulation, the wave velocity in water was 1500 m/s, which was similar to the shear wave velocities. This possibly results in the small effects of bone shape on the shear wave velocity measurement. The averaged shear wave velocities in Fig.5 were 1820 m/s in the inflamed part, 2060 m/s in the normal part. These averaged shear wave velocities were similar to the velocities set in this simulation model. The results show that shear wave may become a good factor to evaluate inflammation and is not strongly affected by the bone shape.

5. conclusion

The applicability of an AT technique to shear wave evaluation was investigated for the horse bone by the FDTD simulation. The observed shear wave velocities were almost independent of the bone surface shape. Averaged velocities in the inflamed part were lower than those of the normal part. These data show that inflammation may be detected by the shear AT technique clinically.

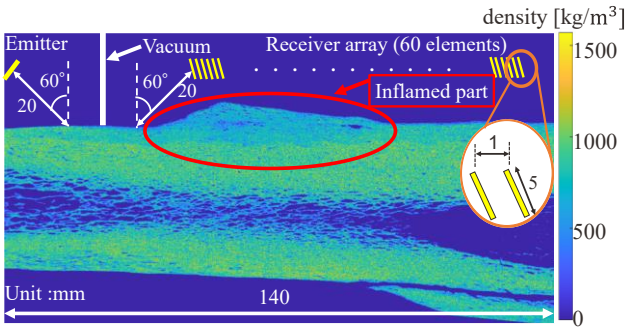

Fig.2 Simulation condition.

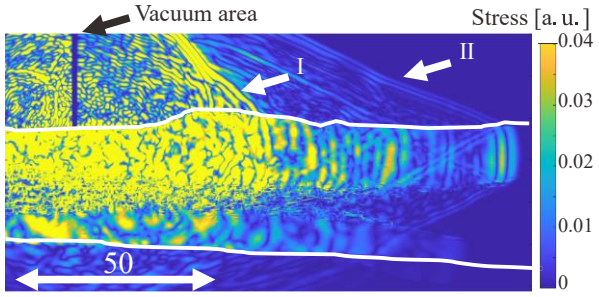

Fig.3 Sound field at 40 μs after wave radiation.

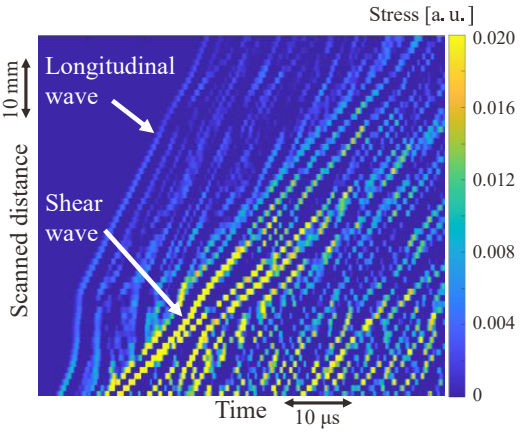

Fig.4 B-scan image.

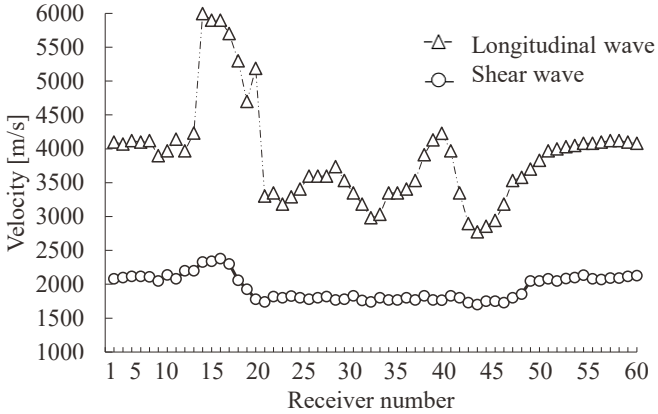

Fig.5 Wave velocities between adjacent receivers.

Reference

1. P. Laugier and G.Haiat eds., Springer (2011).
2. M. Talmant, et al., Ultrasound Med. Biol., **35** (2009) 912.
3. M. Takata et al., Proc. Urtlasonic Symp. (2020).
4. F. N. Fritsch, et al., SIAM J. Numerical Analysis, **17** (1980) 238.
5. T. H. Smit et al., J, Biomech, **35**, Issue 6 (2002) 829.
6. T. Nakatsuji, et al., Jpn. J. Appl. Phys., **50**, 07HF18 (2011).
7. Y. Yamato, et al., Calcif Tissue Int., **82** (2008) 169.
8. Y. Nagatani, et al., Jpn. J. Appl. Phys., **45**, 7186.(2006)
9. B. Leslie et al., Jpn. J. Appl. Phys., **58**, SGGE20(2019).